

# Running in circles: is practical application feasible for data fission and data thinning in post-clustering differential analysis?

Benjamin Hivert

Univ. Bordeaux, INSERM, INRIA, SISTM team, BPH,  
Vaccine Research Institute, VRI, Hôpital Henri Mondor,

Denis Agniel

RAND Corporation,

Rodolphe Thiébaud

Univ. Bordeaux, INSERM, INRIA, SISTM team, BPH,  
CHU Bordeaux, Service d'information médicale,

Vaccine Research Institute, VRI, Hôpital Henri Mondor,

and

Boris P. Hejblum

Univ. Bordeaux, INSERM, INRIA, SISTM team, BPH,

Vaccine Research Institute, VRI, Hôpital Henri Mondor

May 24, 2024

## Abstract

The standard pipeline to analyse single-cell RNA sequencing (scRNA-seq) often involves two steps : clustering and Differential Expression Analysis (DEA) to annotate cell populations based on gene expression. However, using clustering results for data-driven hypothesis formulation compromises statistical properties, especially Type I error control. Data fission was introduced to split the information contained in each observation into two independent parts that can be used for clustering and testing. However, data fission was originally designed for non-mixture distributions, and adapting it for mixtures requires knowledge of the unknown clustering structure to estimate component-specific scale parameters. As components are typically unavailable in practice, scale parameter estimators often exhibit bias. We explicitly quantify how this bias affects subsequent post-clustering differential analysis Type I error rate despite employing data fission. In response, we propose a novel approach that involves modeling each observation as a realization of its distribution, with scale parameters estimated non-parametrically. Simulations study showcase the efficacy of our method when component are clearly separated. However, the level of separability

required to reach good performance presents complexities in its application to real scRNA-seq data.

*Keywords:* Unsupervised learning, Mixture Model, Post-clustering inference, Type I error, Non-parametric estimation, local variance

# 1 Introduction

Clustering encompasses all unsupervised statistical methods that group observations into homogeneous and separated clusters. Widely used in various application fields such as biology or genomics (Jaeger & Banks 2023), clustering plays a significant role to uncover or summarise signals contained in different kind of multivariate data. In the context of single-cell RNA-seq (scRNA-seq) technologies which are high-throughput genomics techniques that measure gene expression at the single-cell level, providing insights into cellular heterogeneity and functional diversity within complex biological tissues, cluster analysis is an integral component of the traditional pipeline for data analysis (Amezquita et al. 2020). Combined with differential expression analysis, it allows to identify and annotate cellular subpopulations by simply grouping cells based on their gene expression. Differential expression analysis tests each individual gene for differential expression between two clusters, leading to the identification of marker genes that could potentially serve as cell-type marker genes (Pullin & McCarthy 2024).

However, such a two-step pipeline for post-clustering differential analysis requires using the same data twice: first to estimate the clusters, and then again to estimate the differences between them and perform significance testing – a procedure sometimes referred to as “double-dipping” (Kriegeskorte et al. 2009). In post-clustering differential analysis, it has been shown that the primary risk of double dipping is to compromise the control of the Type I error rate of otherwise well-calibrated testing procedure for traditional differential analysis, leading to false positives (Zhang et al. 2019). Fundamentally, uncertainties stemming from cluster analysis outcomes, particularly related with determining the optimal number of clusters, could create artificial differences between homogeneous groups of observations. Failure to account for the double use of the data during the analysis may lead

differential analysis tools to erroneously identify those artificial differences (Hivert, Agniel, Thiébaud & Hejblum 2024). Although challenges related to double dipping are increasingly studied, emphasizing their critical importance, they remain unresolved in the context of scRNA-seq data analysis (Lähnemann et al. 2020).

Leveraging the selective inference framework (Fithian et al. 2014), which involves conditioning on the clustering event during the derivation of the test statistic and the associated p-value, various methodological efforts have been carried to address this double dipping issue in post-clustering inference (Gao et al. 2022). Zhang et al. (2019) introduced the Truncated-Normal test (TN-test), a four-step post-clustering differential analysis procedure that involves splitting the data into two parts, followed by cluster analysis on the first part of the data. Subsequently, a support vector machine (SVM) classifier is applied to the clustered data to learn the clustering structure and predict the cluster labels on the remaining data. Finally, a differential analysis is conducted between the predicted clusters using a truncated-normal test. This truncation, on either side of the hyperplane fitted by the SVM, allows to correct for the double dipping issue. However, information loss may occur as an inherent consequence of the data-splitting process. Moreover, the method involves multiple steps, introducing complexity into the overall analytical framework, and Song et al. (2023) highlighted the poor performances of the TN-test in their numerical simulations. More recently, Hivert, Agniel, Thiébaud & Hejblum (2024) and Chen & Gao (2023) have introduced selective tests tailored to detect mean differences between two clusters on individual variables. These methods explicitly condition on the clustering event to derive their p-value, relying on the set of all perturbed data sets that would yield the same partition when subjected to the same clustering algorithm. Hivert, Agniel, Thiébaud & Hejblum (2024) rely on a Monte Carlo approach to suit any clustering algorithm,

which comes at the expense of extensive computational times. On the other hand, Chen & Gao (2023) explicitly describe this set specifically for K-means and hierarchical clustering applied to the squared distance matrix. Bachoc et al. (2023) introduced a selective tests designed for convex clustering. All these proposed selective methods designed for post-clustering inference either require specific clustering algorithms or introduce new specific test statistics. This consequently increases their complexity and makes their application less straightforward in the context of scRNA-seq data analysis.

Leiner et al. (2023) have drawn inspiration from data splitting (which effectively addresses overfitting issues in machine learning) to break free from the selective inference framework. They propose a method called “data fission”, wherein the information within each individual observation is split into two independent parts. The first part could be used for cluster analysis, and labeling observations on the second part simply by matching them to their first counterpart. Differential analysis could then be conducted on the remaining information, *i.e.* the second part. However, in the context of post-clustering differential analysis, it is imperative that the two parts be independent, as each analysis (cluster analysis and differential analysis) must be performed independently to effectively prevent double dipping and the associated inflation of Type I error. Data fission requires strong parametric distributional assumptions, with only the Gaussian and Poisson (Neufeld et al. 2024) distributions ensuring independence between the two fissioned parts. Expanding upon this concept, Neufeld, Dharamshi, Gao & Witten (2023) have generalized the fission process by introducing “data thinning”. Building on the same foundational idea, they not only succeed in developing a process capable of decomposing data into more than two parts, but also broaden the spectrum of distributions where independence between each part is provided. This includes the negative binomial distribution, widely used when modeling

RNA-seq data.

Data fission or data thinning, although initially appealing, present significant limitations. First, these methods lack results and justification when applied to mixture distributions, which are commonly used to model data with a clustered structure (MacQueen et al. 1967). Consequently, the absence of such results inherently assumes a global null hypothesis of no clusters in the data. Additionally, these methods assume prior knowledge of parameters (e.g., variance for the Gaussian distribution or overdispersion for the negative binomial distribution). Although robust estimators for these parameters could theoretically ensure the validity of the method, this further adds complexity for clustered data where each cluster has a different parameter value. And in the absence of knowledge about the data structure, specifically the clusters, the only justifiable estimator is the full-sample one (*i.e.* computed using all the observations regardless of their mixture component), even though it fails to correctly estimate the intra-component parameter value.

Data fission and data thinning have emerged as promising alternatives to selective inference for post-clustering inference, owing to their compatibility with any clustering methods and differential analysis tests. In this article, we propose a strategy to address their inherent limitations by modeling each observation as a realization from distinct random variables with their own parameter value. This approach facilitates the application of fission or thinning processes within the context of mixture distributions although the accurate estimation of scale parameters still remains challenging. We establish a link between the bias in the estimation of the variance parameter in the Gaussian distribution and the expected Type I error rate of the two-sample  $t$ -test (Welch 1947), underscoring the critical importance of a robust estimator and the practical complexities associated with implementing these methods. To tackle this issue, we introduce a non-parametric method for estimating the

local individual variance to be used in the Gaussian setting.

## 2 Methods

In the following, capital letters represent random variables with a probability distribution function denoted as  $p$ ,  $x_i$  denotes a set of  $n$  realizations of  $X$ , and matrices and vectors are bolden.

### 2.1 Data fission and data thinning

Let  $\mathbf{X}$  be a random variable with a known distribution. Both data fission (Leiner et al. 2023) and its generalization, data thinning (Neufeld, Dharamshi, Gao & Witten 2023), aim to decompose the random variable  $\mathbf{X}$  into two (or more in the case of data thinning) new random variables  $\mathbf{X}^{(1)}$  and  $\mathbf{X}^{(2)}$ . These new variables are designed to i) retain information from the original variable  $\mathbf{X}$ , and ii) be independent. Of note, data fission can generate pairs of  $\mathbf{X}^{(1)}$  and  $\mathbf{X}^{(2)}$  that are not independent, but here we will focus on the independent cases only. The balance between the amount of information from  $\mathbf{X}$  kept into either  $\mathbf{X}^{(1)}$  or  $\mathbf{X}^{(2)}$  is tuned by a hyperparameter  $\tau$ . Such a decomposition can be performed for various probability distributions of  $\mathbf{X}$ . For data fission, Leiner et al. (2023) identified only two distributions, the Gaussian and the Poisson, that satisfy the independence requirement. In contrast, Neufeld, Dharamshi, Gao & Witten (2023) established a comprehensive decomposition that ensures independence for all convolution-closed distributions. This encompasses Gaussian, Poisson (Neufeld et al. 2024) and Negative Binomial (Neufeld, Popp, Gao, Battle & Witten 2023) distributions. Decompositions for the three distributions into two independent random variables  $\mathbf{X}^{(1)}$  and  $\mathbf{X}^{(2)}$ , are detailed in Table 1. For proofs of independence, please refer to the Appendix A for the Gaussian case, and to Neufeld et al. (2024) and

Distribution of $\mathbf{X}$	$\tau$	Data fission	Data thinning
		$Z \sim \text{Binom}(X, \tau)$	
$\mathcal{P}(\lambda)$	$\tau \in [0, 1]$	$X^{(1)} = Z$	$X^{(1)}   X = x \sim \text{Binom}(x, \tau)$
		$X^{(2)} = X - Z$	$X^{(2)} = X - X^{(1)}$
		$\mathbf{Z} \sim \mathcal{N}(\mathbf{0}_p, \Sigma_{p \times p})$	
$\mathcal{N}(\boldsymbol{\mu}_p, \Sigma_{p \times p})$	$\tau \in ]0, +\infty)$	$\mathbf{X}^{(1)} = \mathbf{X} + \tau \mathbf{Z}$	$\mathbf{X}^{(1)}   \mathbf{X} = \mathbf{x} \sim \mathcal{N}(\tau \mathbf{x}, \tau(1 - \tau)\Sigma_{p \times p})$
		$\mathbf{X}^{(2)} = \mathbf{X} - \frac{1}{\tau} \mathbf{Z}$	$\mathbf{X}^{(2)} = \mathbf{X} - \mathbf{X}^{(1)}$
$\mathcal{NB}(\mu, \theta)$	$\tau \in [0, 1]$	No fission	$X^{(1)}   X = x \sim \text{BetaBin}(x, \tau\theta, (1 - \tau)\theta)$
			$X^{(2)} = X - X^{(1)}$

Table 1: Data fission and data thinning decompositions for three usual distributions: Poisson, Gaussian and Negative Binomial.

Neufeld, Popp, Gao, Battle & Witten (2023) for the Poisson and negative binomial distribution, respectively. Both Gaussian and negative binomial data fissions/thinnings require knowledge of scale parameters (namely  $\Sigma$  or  $\theta$ ) for practical feasibility, as highlighted in Table 1. Theoretical guarantees, and especially the independence between  $\mathbf{X}^{(1)}$  and  $\mathbf{X}^{(2)}$ , are based on using the true values of these parameters. Yet, in real-life applications these are unknown and need to be estimated, most likely from the data as described in Neufeld, Popp, Gao, Battle & Witten (2023).

## 2.2 Limits in practical application of data fission and data thinning

### 2.2.1 Mixture distributions

Neufeld et al. (2024) and Neufeld, Popp, Gao, Battle & Witten (2023) have proposed the application of data thinning for post-clustering inference. Existing decompositions are currently limited to non-mixture distributions. Unfortunately, these distributions can only



describe a global null hypothesis, assuming the absence of separated clusters within the data. In scenarios with true clusters, a more appropriate modeling approach involves the use of mixture models (Bouveyron et al. 2019) – each component of the mixture representing a distinct cluster. Given  $n$  i.i.d. realizations of random variables following a mixture of distributions, the density function for an observation  $\mathbf{x}_i$  is:  $p(\mathbf{x}_i) = \sum_{k=1}^K \pi_k f(\mathbf{x}_i | \boldsymbol{\theta}_k)$ , where  $\pi_k$  is the probability that an observation was generated by the  $k^{\text{th}}$  component and  $f(\cdot | \boldsymbol{\theta}_k)$  is the density of the  $k^{\text{th}}$  component with its specific parameters  $\boldsymbol{\theta}_k$  (for simplicity, we only consider the case where all components belong to the same parametric distribution with density  $f$ ). Data fission and data thinning assume a homogeneous distribution for all observations, so they are only applicable to one component. In the case of a mixture, they can thus only be applied to each component separately.

Data fission and data thinning therefore create a circular situation, as illustrated in the schematic Figure 1. To be applied for post-clustering inference, these methods require knowledge of the intra-component parameters  $\boldsymbol{\theta}_k$  which, in turn, depend themselves on the components that we would estimate. An effective approach could be to estimate a global parameter  $\hat{\boldsymbol{\theta}}$  based on all observations. However, this would make the critical assumption that the parameter value is the same across all components, *i.e.*  $\boldsymbol{\theta} = \boldsymbol{\theta}_k$ ; this means that the data are distributed according to the same distribution globally, regardless of their component:

$$p(\mathbf{x}_i) = f(\mathbf{x}_i | \boldsymbol{\theta}_k) = f(\mathbf{x}_i | \boldsymbol{\theta}). \quad (1)$$

This can thus only be verified for  $K = 1$ , so under the global null of no cluster. Yun & Foygel Barber (2023) highlighted similar challenges for existing post-clustering selective tests.

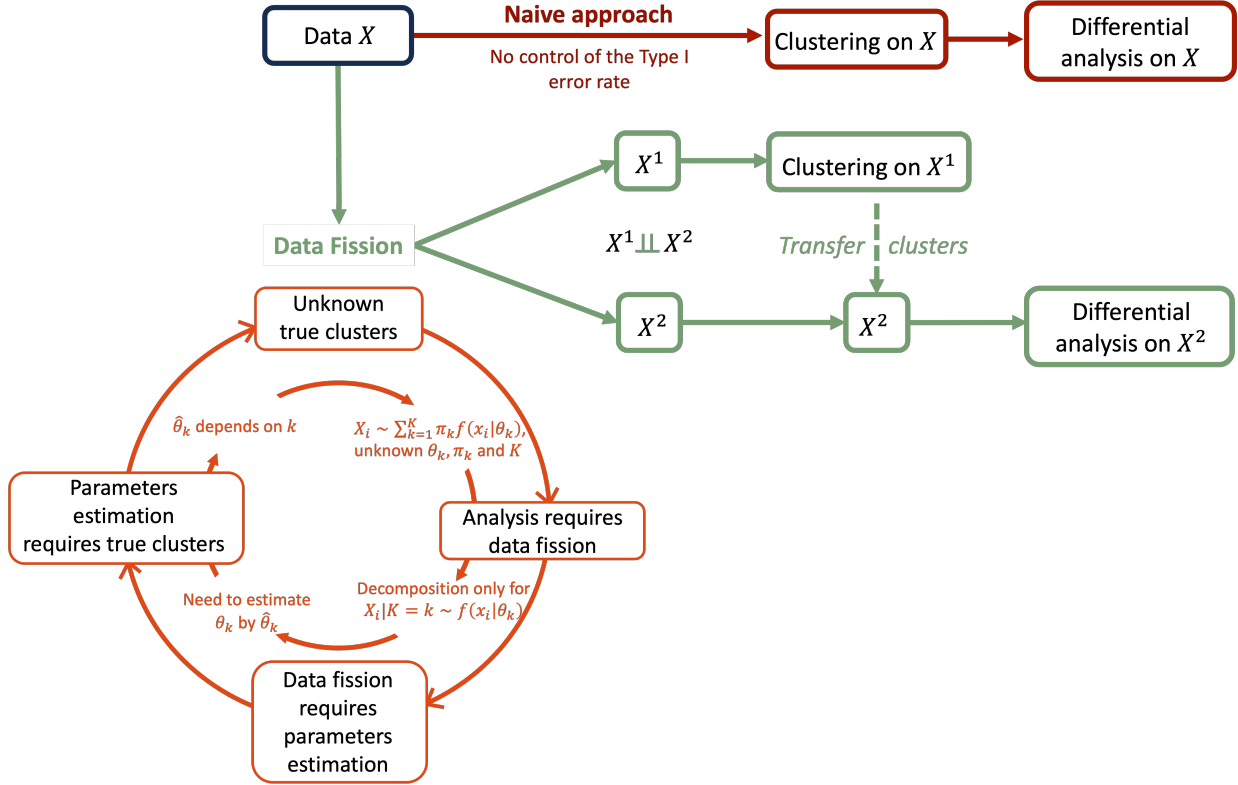


Figure 1: Schematic view illustrating the circularity induced by data fission for post-clustering differential analysis

### 2.2.2 Scale parameter prior knowledge and estimation

We will restrict our analysis to the Gaussian setting, that is considering:

$$f(\mathbf{x}_i | \boldsymbol{\mu}_k, \boldsymbol{\Sigma}_k) = \frac{1}{(2\pi)^{p/2} |\boldsymbol{\Sigma}_k|^{1/2}} \exp\left(-\frac{1}{2}(\mathbf{x}_i - \boldsymbol{\mu}_k)^T \boldsymbol{\Sigma}_k^{-1} (\mathbf{x}_i - \boldsymbol{\mu}_k)\right)$$

with  $k = 1, \dots, K$ ,  $K \geq 1$  the number of components in the mixture, and  $\boldsymbol{\mu}_k \in \mathbb{R}^p$  and  $\boldsymbol{\Sigma}_k \in \mathbb{R}^{p \times p}$  respectively the mean vector and the covariance matrix of the  $k^{\text{th}}$  components. Much of the results apply to the negative binomial case, with the overdispersion parameter being analogous to the variance parameter in the Gaussian case. In this setting, the challenge lies in estimating  $\boldsymbol{\Sigma}_k$  for data fission or data thinning.

Figure 2 provides a comprehensive overview of the challenges associated with variance estimation in data fission. Panel A presents an illustrative example involving 300 real-

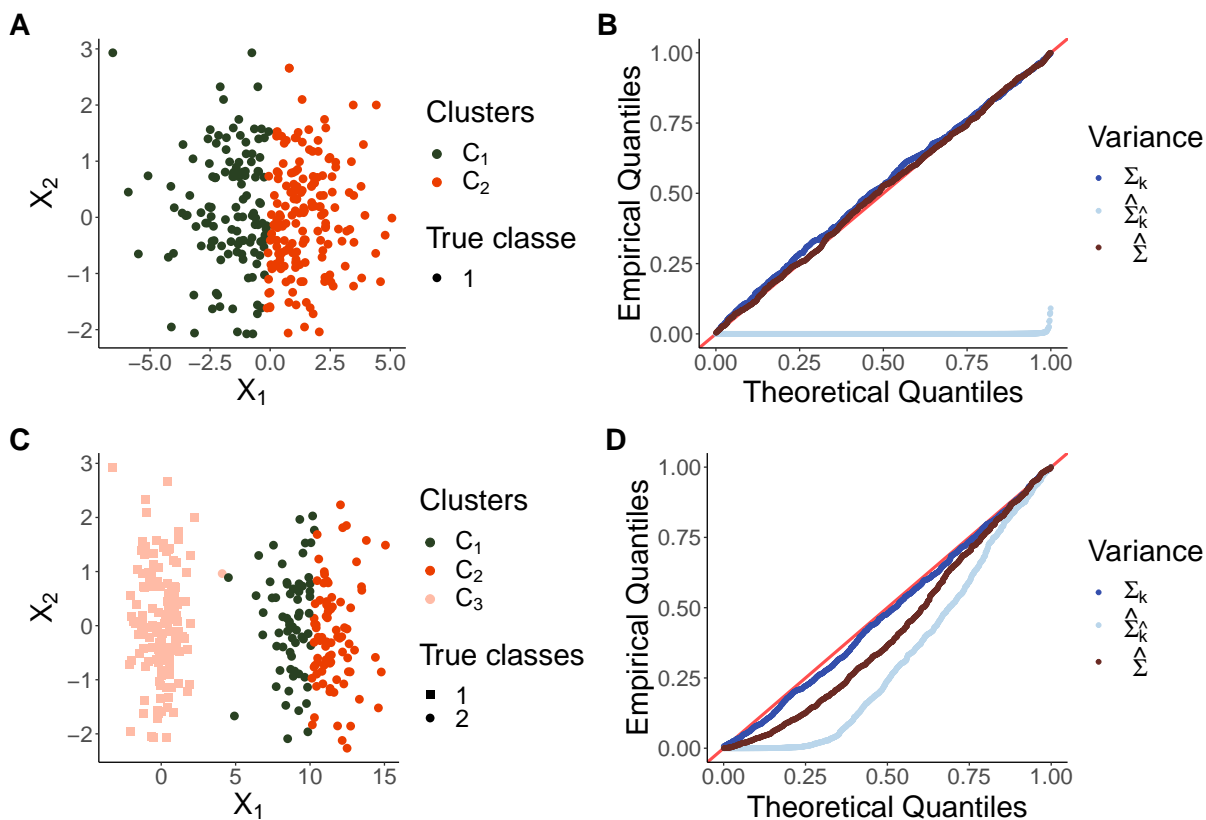


Figure 2: **Toy example illustrating the impact of variance estimation on data fission p-values** **Panel A:** A two-dimensional Gaussian distribution incorrectly clustered into 2 clusters. **Panel B:** QQ-plot of the  $t$ -test p-values for the comparison between the two estimated clusters across 1,000 simulations when data fission is performed with 3 different variance estimators. **Panel C:** Extension of the problem to a two-component, two-dimensional Gaussian mixture incorrectly clustered into 3 clusters.  $C_1$  and  $C_2$  originate from the same component, which is erroneously split into two. **Panel D:**  $t$ -test p-values for the comparison between  $C_1$  and  $C_2$  over 1,000 data simulations using the same 3 variance estimators for the data fission.

izations of a multivariate Gaussian distribution ( $K = 1$ ) with a mean vector  $\boldsymbol{\mu} = \begin{pmatrix} 0 \\ 0 \end{pmatrix}$  and a covariance matrix  $\boldsymbol{\Sigma} = \begin{pmatrix} 4 & 0 \\ 0 & 1 \end{pmatrix}$ . The k-means algorithm was applied to this dataset, resulting in the estimation of two clusters,  $C_1$  and  $C_2$ . Data fission performance was evaluated when using different estimations of  $\boldsymbol{\Sigma}$ . First, we considered the true intra-components covariance matrix  $\boldsymbol{\Sigma}_k$  (see section 2.3.1 for a proposed approach to data fission assuming several mixture component). We also considered the overall sample covariance matrix  $\widehat{\boldsymbol{\Sigma}} = \frac{1}{n-1} \sum_{i=1}^n (\mathbf{x}_i - \overline{\mathbf{X}}) (\mathbf{x}_i - \overline{\mathbf{X}})^t$  where  $\overline{\mathbf{X}}$  is the sample mean vector. We finally use the  $k$ -means results to compute an intra-cluster covariance matrix defined as:  $\widehat{\boldsymbol{\Sigma}}_k = \frac{1}{|C_k|-1} \sum_{i=1 \in C_k} (\mathbf{x}_i - \overline{\mathbf{X}}_{C_k}) (\mathbf{x}_i - \overline{\mathbf{X}}_{C_k})^t$  where  $\overline{\mathbf{X}}_{C_k}$  is the sample mean vector of the cluster  $C_k$ . Since both clusters originate from the same component, there is no inherent differences between them, implying that the  $t$ -test p-values should exhibit a uniform distribution. Panel **B** presents a QQ-plot illustrating the resulting p-values against the Uniform distribution for the test on  $X_1$  in 1,000 replications of the experiment. In this scenario where the mixture has only one component ( $K = 1$ ), the sample covariance matrix  $\widehat{\boldsymbol{\Sigma}}$  provides an unbiased estimate of the true  $\boldsymbol{\Sigma}$ , resulting in uniformly distributed p-values. However, when considering the intra-cluster covariance matrices  $\widehat{\boldsymbol{\Sigma}}_k$  (for  $k = 1, 2$ ) derived from the k-means results, the p-values no longer exhibit a uniform distribution. In this case, the estimated matrices  $\widehat{\boldsymbol{\Sigma}}_k$  for each cluster drastically underestimate the true covariance matrix  $\boldsymbol{\Sigma}$ , compromising the independence between  $\mathbf{X}^{(1)}$  and  $\mathbf{X}^{(2)}$ . This deviation from independence indicates that it becomes straightforward to replicate the clusters identified in  $\mathbf{X}^{(1)}$  onto  $\mathbf{X}^{(2)}$ .

Panel **C** introduces a scenario with two true clusters generated using a mixture of two Gaussian distributions ( $K = 2$ ). The K-means identifies 3 clusters (for illustration purposes), incorrectly splitting one mixture component into clusters  $C_1$  and  $C_2$ . We compared

data fission performance was again compared when the decomposition is performed using the same 3 covariance estimators as in the previous scenario. Panel **D** presents the resulting p-values for the  $t$ -test on  $C_1$  and  $C_2$  on  $X_1$  over 1,000 replications of the analysis. Efficient Type I error control is achievable only by considering the true intra-components covariance matrix. Both global and estimated intra-cluster covariances are biased estimators, leading to correlations between  $\mathbf{X}^{(1)}$  and  $\mathbf{X}^{(2)}$ , compromising control of the Type I error rate. This underscores the intricate challenges associated with covariance estimation for data fission in practical scenarios, mainly due to the misspecification of the generative model for data fission arising when genuine clusters exist within the dataset.

## 2.3 Practical solutions

### 2.3.1 Individual fission (or thinning) for mixture models

In Gaussian mixture models, parameters are typically component-specific, meaning that they are assumed to be shared across all individuals within each component. As explained above and in Figure 1, this assumption poses a circular challenge as it requires knowledge of the true data structure to be able to accurately estimate the component-specific covariance matrices that are then needed to perform data fission or data thinning. To address this limitation, we propose an alternative approach in which each observation is modeled as a realization of its own Gaussian distribution, *i.e.*  $p_i(\mathbf{x}_i) = f(\mathbf{x}_i | \boldsymbol{\mu}_i, \boldsymbol{\Sigma}_i)$ . Thus, observations are no longer assumed to be identically distributed). Consequently, the covariance matrix  $\boldsymbol{\Sigma}_i$  is no longer specific to the components but instead to the individual observations. Despite this individual-level definition, two individuals drawn from the same component are expected to have very close variance parameters. By bypassing the components in the definition of  $\boldsymbol{\Sigma}_i$ , this modeling strategy theoretically encompasses both the global null

( $K = 1$ ) and the mixture ( $K \geq 1$ ) settings, and opens up individual-level data fission and data thinning. As highlighted above, variance estimation remains crucial for the practical feasibility of these methods. This new modeling assumes individual variances that still need to be known (ideally), or precisely estimated in real-life settings.

### 2.3.2 Non-parametric local variance estimation

To estimate  $\Sigma_i$ , we propose to use weighted variances where the weights are determined through non-parametric estimations using kernel smoothing. The underlying principle behind this approach is that, despite the individual-specific nature of the variance, two observations within the same component of the mixture (i.e., two neighbors) should display similar variance patterns. The non-parametric weights assigned to each individual reflect their contribution to the estimation of the variance for the  $i^{\text{th}}$  observation, effectively capturing the proximity between individuals. First, let's assume that we are under the univariate setting, that is:  $X_i \sim \mathcal{N}(\mu_i, \sigma_i^2)$  for  $i = 1, \dots, n$ . We define  $\hat{\sigma}_i^2$ , the resulting estimate of  $\sigma_i^2$ , as:

$$\hat{\sigma}_i^2 = \frac{\sum_{j=1}^n w_{ij} (x_i - \hat{m}_i)^2}{\left(\sum_{j=1}^n w_{ij}\right) - 1} \quad (2)$$

where  $w_{ij}$  are individual-weights and  $\hat{m}_i = \sum_{j=1}^n w_{ij} x_j / \sum_{j=1}^n w_{ij}$  are individual-specific weighted means. Ideally,  $w_{ij}$  should be zero (or very small) for all the observations  $x_j$  that are not in the same component as  $x_i$ .

The catch of the variance computation in (2) lies in determining each individual weight  $w_{ij}$ . Since it is essential for  $w_{ij}$  to appropriately capture the proximity between observations, we opted for a kernel-based definition:  $w_{ij} = K(x_i - x_j)$ , where  $K(u) = \frac{1}{\sqrt{2\pi}h} e^{-\frac{u^2}{2h^2}}$

represents the uniform kernel providing the proximity measurement between  $x_i$  and  $x_j$ . This ensures that individual weights reflect the local relationships within the data. This kernel choice focuses on nearby points, emphasizing their influence on the weighted variance estimate. The parameter  $h$  in the definition of  $K$  serves as the bandwidth parameter, controlling the width of the kernel and, consequently, the neighborhood around each observation  $x_i$  that contributes to its weighted variance estimate. A smaller  $h$  results in more localized estimations, emphasizing nearby points, but can lead to underestimate the variances. Conversely, a larger  $h$  includes a broader range of observations, and an excessively large value might consider almost all observations in the variance estimation, yielding an estimator close to the full sample one. Therefore, an optimal choice for  $h$  would involve considering only the observations in the same components of the underlying mixture. However, achieving this ideal scenario is impractical as it is equivalent to knowing the true components of the mixture.

Bandwidth calibration is a crucial step in any kernel method (Heidenreich et al. 2013). We propose to use individual-specific bandwidth  $h_i = h(x_i)$  to reduce the bias in kernel density estimation. To accomplish this, we first estimate the changepoint,  $i^*$  in the spread of distances from observation  $x_i$  to all other observations. This changepoint delineates the change in components of the mixture: observations with distances preceding this changepoint are deemed part of the same component as  $x_i$ , whereas those following it are considered part of different components. Subsequently, we define  $h_i = |x_i - x_{i^*}|$  as the distance between  $x_i$  and the observation  $x_{i^*}$  that is furthest from  $x_i$  before the break in the mixture. Thus,  $h_i$  is determined in such a way that the individual bandwidth accommodates only the observations in the same component as  $x_i$ , ensuring its size is sufficient to encompass all observations of the component (Chacón & Duong 2020).

### 3 Results

#### 3.1 Quantification of Type I error rate as a function of the bias in the variance estimation

Independence between  $\mathbf{X}^{(1)}$  and  $\mathbf{X}^{(2)}$  is guaranteed solely when the true variance is used for decomposition. Substituting the true variance  $\Sigma_i$  with an estimate  $\widehat{\Sigma}_i$  introduces correlations between these new random variables. Consider a Gaussian random variable  $\mathbf{X} \sim \mathcal{N}(\boldsymbol{\mu}_p, \Sigma_{p \times p})$  that we aim to decompose using the data fission or data thinning processes outlined in Table 1, but with an estimated covariance matrix,  $\widehat{\Sigma}$ , in place of  $\Sigma$ . Table 2 provides the covariance values between  $\mathbf{X}^{(1)}$  and  $\mathbf{X}^{(2)}$  as a function of the bias of  $\widehat{\Sigma}$  (for proofs, refer to Appendix B for data fission and to Neufeld, Dharamshi, Gao & Witten (2023) for data thinning). If  $\mathbf{X}^{(1)}$  and  $\mathbf{X}^{(2)}$  are not independent (as with a biased estimator of  $\Sigma$  that induces significant covariance), a split of a single component into two estimated clusters in  $\mathbf{X}^{(1)}$  is easily transferred to  $\mathbf{X}^{(2)}$  and results in false positives during the inference step (even if the latter is carried out on  $\mathbf{X}^{(2)}$ ).

	<b>Data Fission</b>	<b>Data Thinning</b>
$\text{Cov}(\mathbf{X}^{(1)}, \mathbf{X}^{(2)})$	$\Sigma - \widehat{\Sigma}$	$\tau(1 - \tau)(\Sigma - \widehat{\Sigma})$

Table 2: Bias in the estimation of  $\Sigma$  induces correlations between  $\mathbf{X}^{(1)}$  and  $\mathbf{X}^{(2)}$

To further describe the repercussions of variance estimation in the context of data fission, we derived an analytical expression for the Type I error rate of the  $t$ -test as a function of the bias in estimating this parameter. Let  $X \sim \mathcal{N}(\mu, \sigma^2)$  be a random variable. Given that  $X$  is not generated from a mixture of distributions, it becomes evident that distinct clusters are not inherent in the variable. Our aim is to perform data fission in  $X$ , using  $X^{(1)}$  for  $k$ -means clustering (with  $K = 2$ ) and  $X^{(2)}$  for differential testing between



the two inferred clusters. Notably, we employ an estimate  $\widehat{\sigma}^2$  of  $\sigma^2$  in the fission process. Given the generation process of  $X$ , it is established that regardless of the clustering on  $X^{(1)}$ , there should be no mean difference between the estimated clusters on  $X^{(2)}$  as long as independence is achieved. Let  $\widehat{C}_1$  and  $\widehat{C}_2$  be the two estimated clusters on  $X^{(1)}$  with the same intra-cluster variance, which is a reasonable hypothesis with  $k$ -means clustering as explained in Appendix C. Since we are under the null hypothesis of no mean difference between the clusters, the  $T$  statistic for the  $t$ -test between  $\widehat{C}_1$  and  $\widehat{C}_2$  on  $X^{(2)}$  is given by:

$$T_{\widehat{C}_1, \widehat{C}_2} = \frac{\widehat{\delta}_{X^{(2)}}}{\sqrt{\frac{4s^2(X^{(2)})}{n}}} \quad (3)$$

Here,  $\widehat{\delta}_{X^{(2)}}$  represents the observed mean difference between  $\widehat{C}_1$  and  $\widehat{C}_2$  on  $X^{(2)}$  and  $s^2(X^{(2)})$  is their shared intra-cluster variance. Of note,  $\widehat{\delta}_{X^{(2)}}$  and  $s^2(X^{(2)})$  both depend on the ability to reproduce the clustering results obtained on  $X^{(1)}$  into  $X^{(2)}$ . This is quantified by their correlation  $\text{Cor}(X^{(1)}, X^{(2)})$ , which can be easily computed from their covariance given in Table 2. Based on this correlation, it can be demonstrated that:

$$T_{\widehat{C}_1, \widehat{C}_2} \stackrel{\mathcal{H}_0}{\sim} \mathcal{N} \left( \frac{\sqrt{n} \sqrt{\frac{2}{\pi} \text{Cor}(X^{(1)}, X^{(2)})^2}}{\sqrt{1 - \frac{2}{\pi} \text{Cor}(X^{(1)}, X^{(2)})^2}}, 1 \right)$$

where  $\text{Cor}(X^{(1)}, X^{(2)}) = \frac{(\sigma^2 - \widehat{\sigma}^2)}{\sqrt{(\sigma^2 + \tau^2 \widehat{\sigma}^2) \times (\sigma^2 + \frac{1}{\tau^2} \widehat{\sigma}^2)}}$ . Appendix C gives details on the derivation of this test statistic and its distribution. The associated Type I error rate for this test is given by  $1 - F(q_{\alpha/2}) + F(-q_{\alpha/2})$ , where  $F$  is the cumulative distribution function of  $\mathcal{N} \left( \frac{\sqrt{n} \sqrt{\frac{2}{\pi} \text{Cor}(X^{(1)}, X^{(2)})^2}}{\sqrt{1 - \frac{2}{\pi} \text{Cor}(X^{(1)}, X^{(2)})^2}}, 1 \right)$  (or the corresponding non-central  $\mathcal{T}(n - 2)$  distribution), and  $q_{\alpha/2}$  is the quantile of a standard Gaussian distribution  $\mathcal{N}(0, 1)$  (or of a  $\mathcal{T}(n - 2)$  distribution).

We validated this theoretical result through numerical simulations, and conducted a detailed exploration of the influence of variance values and sample size on the resulting Type I error rate. We generated  $n$  realizations of a Gaussian random variable with a mean

$\mu = 0$  and variances  $\sigma^2$ , with 1,000 Monte Carlo repetitions. Subsequently, we used data fission with varying values of  $\hat{\sigma}^2$ , obtaining  $X^{(1)}$  for k-means clustering with  $K = 2$  and  $X^{(2)}$  for testing mean differences between the two estimated clusters. Initially, we examine the impact of the original true variance  $\sigma^2$  by considering  $\sigma^2$  values of  $\{0.01, 1, 4\}$  for a fixed sample size of  $n = 100$ . Figure 3A, illustrates the relationship between the bias in estimating  $\sigma^2$  and the Type I error rate, demonstrating a consistent agreement with the derived theoretical error rate. We further documented the behavior of the Type I error for a fixed  $\sigma^2 = 1$  with varying sample sizes  $n \in \{50, 100, 250, 100, 1000\}$  in Figure 3B, which shows the expected impact of the sample size on the Type I error rate. These findings collectively underscore the critical importance of accurately estimating the variance to achieve a well-calibrated Type I error rate with data fission.

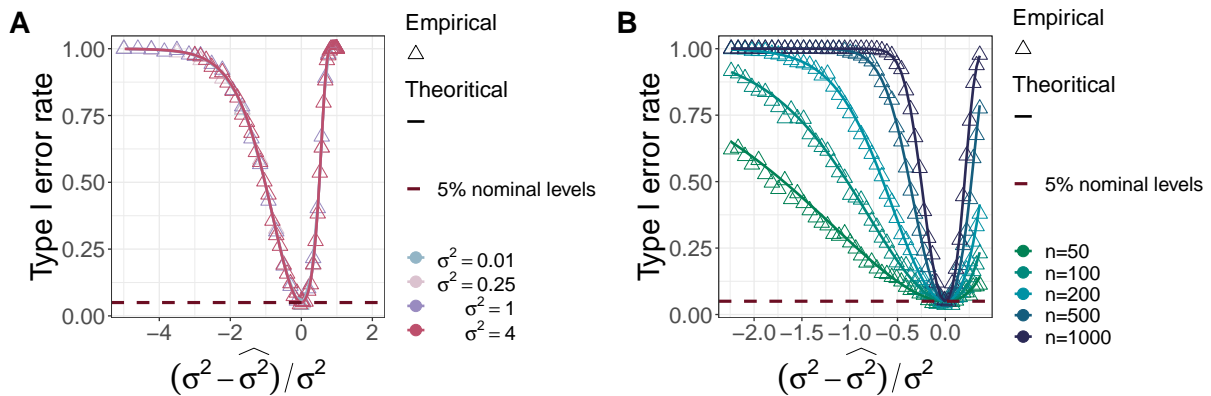


Figure 3: **Impact of variance estimation on Type I error rate in data fission.**

Panel **A**: Evolution of the estimated Type I error rate in data fission as a function of the relative bias and the original variance of the data. Panel **B**: Evolution of the estimated Type I error rate in data fission as a function of the relative bias and the sample size.

## 3.2 Performances of the local variance estimator

We conducted simulation studies to assess the performance of the non-parametric variance estimator defined in (2). Generating univariate data akin to the motivating example in Figure 2 with  $n = 100$  realizations from a two-component univariate Gaussian mixture:  $0.5\mathcal{N}(0, \sigma^2) + 0.5\mathcal{N}(\delta, \sigma^2)$ . We explored a range of ratio  $\delta/\sigma$  values from 0 (*i.e.* no separation between the components, representing the global null of no clusters in the data) to 100 (indicating an extreme separation). Different values of  $\sigma^2$  were considered:  $\sigma^2 \in \{0.01, 1, 4\}$ . For each pair  $(\delta, \sigma^2)$  defining the mixture, variance was estimated from the data using our proposed weighted local variance, and the result was used for individual data fission. We then considered only the observations coming from the first component of the mixture for  $k$ -means clustering on the corresponding  $X^{(1)}$  with  $K = 2$ . This resulted in one true component splitting into two incorrect clusters. We then tested the mean differences between those two clusters using the  $t$ -test on  $X^{(2)}$ . This scenario was replicated 1,000 times, and we computed the empirical Type I error rate at the  $\alpha = 5\%$  level.

Figure 4A shows that local variances are underestimated (manifested as a negative relative bias) until the signal vs. noise ratio  $\delta/\sigma$  reaches approximately 3 – a threshold value for separation in a Gaussian mixture model previously reported in the literature (Siffer et al. 2018, Hivert, Agniel, Thiébaud & Hejblum 2024). Consequently, there are no clear change-points in the spread of distances for individual observations and all observations should contribute significantly to the variance calculation. However, this is not the case here (with a bandwidth  $h_i$  that is too small), leading to underestimated local variances. As the ratio increases within the range  $3.5 \leq \delta/\sigma \leq 10$ , component separation becomes clearer but the identification of change-points remains challenging. Change-points detection is intricate for observations in the tails in-between the components, leading to non-zero

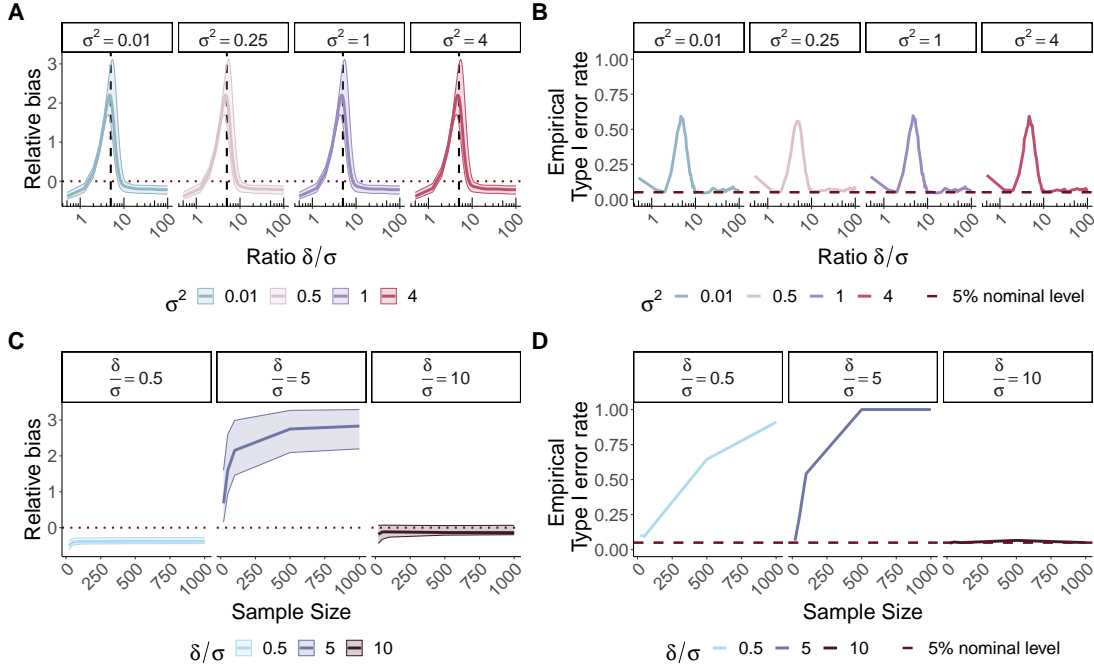


Figure 4: **Performance evaluation of the non-parametric variance estimator in a simulated univariate setting.** All empirical results were obtained through 1,000 simulations of the data. Panel **A**: Median relative bias, defined as  $(\hat{\sigma}^2 - \sigma^2) / \sigma^2$  and its associated inter-quantile range, against the signal-to-noise ratio  $\delta/\sigma$ . Panel **B**: Type I error rate at the  $\alpha = 5\%$  level against  $\delta/\sigma$ . Panel **C**: Median relative bias and its associated inter-quantile range as a function of the sample size for three degrees of separation between the two components (informed by the ratio  $\delta/\sigma$ ). Panel **D**: Type I error rate at the  $\alpha = 5\%$  level as a function of sample size.

weight for observations in both components. Consequently, an overestimation of the local variances (positive relative biases) is observed together with an increase in their associated inter-quantile range. Finally, for  $\delta/\sigma > 10$ , sufficient component separation ensures consistent local variance estimation, highlighting the critical importance of clear-cut component separation for accurate variance estimation. Thus, the methodology outlined in 2.3.2 requires well-separated observations to be able to provide accurate variance estima-

tions. In Figure 4B, the Type I error rate at 5% remains well calibrated only for values of  $\delta/\sigma$  that ensures robust variance estimations (that is  $\delta/\sigma > 10$ ), emphasizing again the necessity of good component separations for reliable testing. Figure 4C demonstrates how increasing the sample size fails to improve non-parametric local variance estimations for three representative values of the ratio  $\delta/\sigma \in \{0.5, 5, 10\}$ , indicating that performance is more dependent upon component separation rather than sample size. The corresponding Type I error rates depicted in Figure 4B thus align with the observed relative bias results, underscoring the critical role of accurate estimation of local variances to ensure Type I error control.

### 3.3 Application to single-cell RNA-seq data analysis

Single-cell RNA-seq (scRNA-seq) data analysis pipelines often involve an initial cluster analysis followed by differential analysis to identify marker genes and annotate cell populations based on gene expression. Given their overdispersed count nature, the negative binomial distribution is favored over the Gaussian distribution to model scRNA-seq data. Unfortunately, the negative binomial distribution also raises challenges for data thinning. The overdispersion parameter  $\theta$  plays a role similar to the variance parameter in the Gaussian distribution, as it is considered known. Therefore, the quality of its estimation is directly impacts  $\text{Cov}(X^{(1)}, X^{(2)}) = \tau(1 - \tau)\frac{\mu^2}{\theta} \left(1 - \frac{\theta+1}{\theta+1}\right)$ , where  $\hat{\theta}$  is an estimated of  $\theta$  (Neufeld, Dharamshi, Gao & Witten 2023). Also, for negative binomial mixtures, data thinning decomposition is once again feasible only at the component level. As the overdispersion parameter is component-specific (Li et al. 2018), providing an estimator that ensures independence is here also a harduous and circular task, given that the components themselves are again unknown and thus require estimation through data thinning.

We further illustrate the necessity of applying intra-component data thinning (with the associated intra-components overdispersion) to ensure Type I error control in the post-clustering inference setting with numerical simulations. We generated  $n = 100$  observations from a two-component negative binomial mixture:  $0.5\text{NegBin}(\mu_1, \theta_1) + 0.5\text{NegBin}(\mu_2, \theta_2)$  with component parameters  $(\mu_1, \theta_1) = (5, 5)$  and  $(\mu_2, \theta_2) = (60, 40)$ . We conducted similar post-clustering inference as in Figure 2. In Figure 5A, applying the  $k$ -means with  $K = 3$  clusters reveals that the first mixture component is erroneously split into 2 clusters (labeled  $C_1$  and  $C_3$ ). We then assessed the Type I error rate associated with the Wilcoxon test between these incorrect clusters when applying data thinning with various overdispersion estimators. First, we applied intra-component data thinning using oracle estimates  $\tilde{\theta}_k$ ,  $k = 1, 2$ , representing true intra-component overdispersion parameters (unfeasible in real-life application where the true cluster structure is unknown). We compared those results with two alternatives that are feasible in practice: i) applying intra-cluster data thinning based on the  $k$ -means results from Figure 5A with their associated  $\hat{\theta}_{\hat{k}}$ ,  $\hat{k} = 1, 2, 3$ , and global data thinning with its associated  $\hat{\theta}$ . Of note, all the overdispersion estimations were performed using Maximum Likelihood. Figure 5B presents the QQ-plot against the Uniform distribution of the associated Wilcoxon p-values across 1,000 simulations. Similarly to the Gaussian setting, achieving uniformly distributed p-values is only possible through intra-component data thinning using their oracle overdispersion estimates  $\tilde{\theta}_k$ . All other data thinning approaches are performed with biased estimators of the overdispersion compromising the independence between  $X^{(1)}$  and  $X^{(2)}$ , and therefore leading to failure in the control of the post-clustering Type I error rate.

Extending our investigation from simulated scenarios to real-life applications, we used a single-cell RNA-seq dataset from the Tabula Sapiens Consortium (Consortium\* et al. 2022)

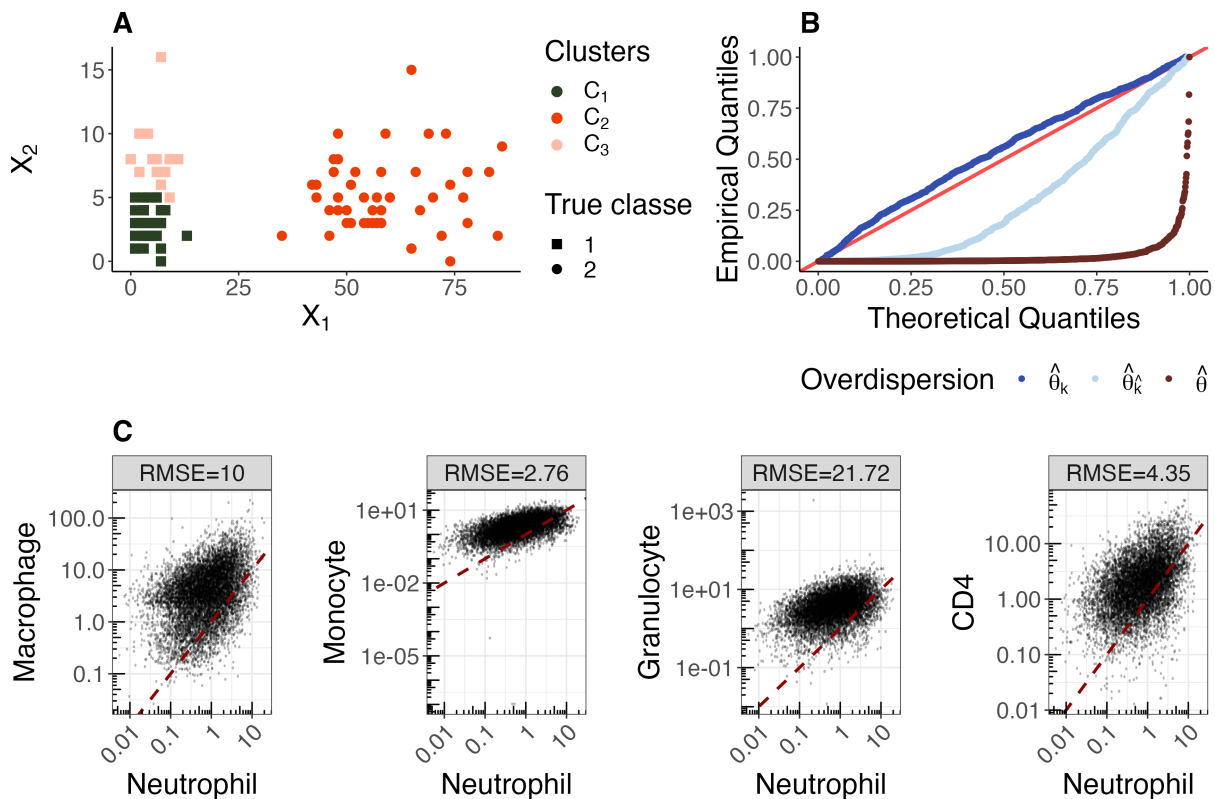


Figure 5: **Challenges in estimating overdispersion, a gene-specific parameter, for negative binomial data thinning.** Panel A showcases erroneous clustering results on a simulated dataset, while Panel B presents a QQ-plot against the Uniform distribution, displaying Wilcoxon p-values from various data thinning approaches over 1,000 simulations when testing between the two erroneous clusters. In Panel C, the estimated overdispersions of genes within different cell populations (macrophages, monocytes, granulocytes, and CD4) are plotted against those in neutrophils, along with their associated Root Mean Square Error (RMSE) for comparison.

to delve into the practical challenges of estimating overdispersion. Our analysis focused on five distinct cell populations: 2,560 neutrophils, 105 macrophages, 386 monocytes, 454 granulocytes, and 833 CD4 T cells – all collected from a single donor. In this controlled setting, where cell types were known, we succeeded in estimating the overdispersion of 8,333

genes for each cell type using the variance stabilizing transformation implemented in the `sctransform` package (Choudhary & Satija 2022). Figure 5C illustrates the comparison of gene overdispersion when estimated solely in neutrophils versus the overdispersion estimated for the same genes in the other four cellular populations. Root Mean Squared Error (RMSE) values were computed to quantify the agreement between estimations. Our findings reveal that overdispersion is specific to each cell population, as evidenced by a notable deviation from the diagonal and relatively high RMSE values. This underscores the challenge of accurately estimating this parameter without prior knowledge of the true mixture underlying the data. Combined with our simulation studies, these results demonstrate how Type I error can easily be inflated in real-life applications of data thinning for scRNA-seq data analysis, particularly due to the difficulty in providing an unbiased estimate of gene overdispersion.

## 4 Discussion

We highlight here the practical limitations inherent in data fission and its extension, data thinning, for post-clustering inference challenges. A crucial issue is the assumption of a homogeneous data distribution, which implies an absence of true clusters in the data. To address this limitation and adapt to scenarios with true classes, a shift towards mixture models becomes imperative. However, these models lack a predefined decomposition through data fission or thinning.

We have proposed an intra-component decomposition for data fission and data thinning, and demonstrated its theoretical validity. It relies on a priori knowledge of the mixture components scale parameters, such as variances in the Gaussian distribution or the overdispersion in the negative binomial distribution. However in real-life applications, these pa-



rameters are unknown. Adequately estimating these parameters becomes intricate in the presence of true clusters, given their component-specific nature ; meanwhile the quality of the estimation of those parameters is directly linked with the covariance between the new random variables,  $X^{(1)}$  and  $X^{(2)}$ , decomposing the original data. Only unbiased estimation of these parameters ensures the independence between  $X^{(1)}$  and  $X^{(2)}$ . That independence is paramount for post-clustering inference to adequately control the Type I error rate.

In the Gaussian framework, we theoretically quantified the relationship between the relative bias in variance estimation and the associated Type I error in post-clustering  $t$ -tests. In practice, our simulation results suggest that a small relative bias can be acceptable while still achieving effective Type I error control. These first results pave the way for defining a principled approach to tuning the hyperparameter  $\tau$  in data fission and data thinning for post-clustering inference to optimize statistical power.

As a solution to avoid the need for prior knowledge of component-specific variance parameters in the Gaussian mixture setting, we propose a heteroscedastic model with individual variances, that can be estimated through a non-parametric weighted estimator. This approach aligns more closely with the distributional assumptions made by data fission and thinning. However, the performance of this non-parametric approach relies heavily on the choice of its bandwidth. The best bandwidth would be the one capturing only the observations originating from a same components, but it would again require knowledge of the true mixture components whereas their estimation is part of the clustering first step of the method.

Finally, we demonstrated that the results derived the Gaussian distribution context are readily applicable to the negative binomial distribution commonly employed in modeling RNA-seq data. Specifically, we illustrate on real data that overdispersion is also component-

specific. Therefore, without knowing the true cluster structure data, data thinning can not ensure the needed independence between clustering and differential testing.

In practice, the application of data fission or data thinning for post-clustering inference appears to be akin to a self-referential loop generating circular reasoning. While introduced as a solution for addressing challenges in post-clustering inference, all strategies that could theoretically ensure independence between the two stages of the analysis ultimately rely on knowledge of the true, but unknown, clusters. Despite its conceptual appeal, the practical utility of these methods for post-clustering inference is remains limited to extreme cases with extremely high signal vs. noise ratios, emphasizing the need for alternative methodologies that can navigate the complexities of unknown class structures more effectively.

All codes and data needed to reproduce the results presented here are openly accessible from Zenodo with DOI 10.5281/zenodo.11207777 (Hivert, Agniel, Thiébaud & Hejblum 2024).

## 5 Acknowledgements

BH is supported partly by the Digital Public Health Graduate’s school, funded by the PIA 3 (Investments for the Future – Project reference: 17-EURE-0019). The work was supported through the DESTRIER Inria Associate-Team from the Inria@SiliconValley program (analytical code: DRI-012215), and by the CARE project funded from the Innovative Medicines Initiative 2 Joint Undertaking (JU) under grant agreement n° IMI2-101005077. The JU receives support from the European Union’s Horizon 2020 research and innovation programme and EFPIA and Bill & Melinda Gates Foundation, Global Health Drug Discovery Institute, University of Dundee. This work has received funding from the European Union’s Horizon 2020 research and innovation programme under EHVA grant agreement n° H2020-

681032. This study was carried out in the framework of the University of Bordeaux's France 2030 program / RRI PHDS. Computer time for this study was provided by the computing facilities MCIA (Mésocentre de Calcul Intensif Aquitain) of the Université de Bordeaux and of the Université de Pau et des Pays de l'Adour.

## References

- Amezquita, R. A., Lun, A. T., Becht, E., Carey, V. J., Carpp, L. N., Geistlinger, L., Marini, F., Rue-Albrecht, K., Risso, D., Sonesson, C. et al. (2020), 'Orchestrating single-cell analysis with bioconductor', *Nature methods* **17**(2), 137–145.
- Bachoc, F., Maugis-Rabusseau, C. & Neuvial, P. (2023), 'Selective inference after convex clustering with  $\ell_1$  penalization', *arXiv preprint arXiv:2309.01492* .
- Bouveyron, C., Celeux, G., Murphy, T. B. & Raftery, A. E. (2019), *Model-based clustering and classification for data science: with applications in R*, Vol. 50, Cambridge University Press.
- Chacón, J. E. & Duong, T. (2020), *Multivariate Kernel Smoothing and Its Applications SMOOTHING AND ITS APPLICATIONS*, CRC PRESS.
- Chen, Y. T. & Gao, L. L. (2023), 'Testing for a difference in means of a single feature after clustering', *arXiv preprint arXiv:2311.16375* .
- Choudhary, S. & Satija, R. (2022), 'Comparison and evaluation of statistical error models for scrna-seq', *Genome Biology* **23**, 20.  
**URL:** <https://doi.org/10.1186/s13059-021-02584-9>
- Consortium\*, T. T. S., Jones, R. C., Karkanas, J., Krasnow, M. A., Pisco, A. O.,

- Quake, S. R., Salzman, J., Yosef, N., Bulthaupt, B., Brown, P. et al. (2022), ‘The tabula sapiens: A multiple-organ, single-cell transcriptomic atlas of humans’, *Science* **376**(6594), eabl4896.
- Fithian, W., Sun, D. & Taylor, J. (2014), ‘Optimal inference after model selection’, *arXiv preprint arXiv:1410.2597*.
- Gao, L. L., Bien, J. & Witten, D. (2022), ‘Selective inference for hierarchical clustering’, *Journal of the American Statistical Association* pp. 1–11.
- Heidenreich, N.-B., Schindler, A. & Sperlich, S. (2013), ‘Bandwidth selection for kernel density estimation: a review of fully automatic selectors’, *AStA Advances in Statistical Analysis* **97**, 403–433.
- Hivert, B., Agniel, D., Thiébaud, R. & Hejblum, B. P. (2024), ‘Post-clustering difference testing: Valid inference and practical considerations with applications to ecological and biological data’, *Computational Statistics & Data Analysis* **193**, 107916.
- Hivert, B., Agniel, D., Thiébaud, R. & Hejblum, B. P. (2024), ‘Reproducible codes and results for Running in circles: is practical application feasible for data fission and data thinning in post-clustering differential analysis? (Version v1) [Data set]’, *Zenodo*. DOI: 10.5281/zenodo.11207777.
- URL:** <https://doi.org/10.5281/zenodo.11207777>
- Jaeger, A. & Banks, D. (2023), ‘Cluster analysis: A modern statistical review’, *Wiley Interdisciplinary Reviews: Computational Statistics* **15**(3), e1597.
- Kriegeskorte, N., Simmons, W. K., Bellgowan, P. S. & Baker, C. I. (2009), ‘Circular analysis

- in systems neuroscience: the dangers of double dipping’, *Nature neuroscience* **12**(5), 535–540.
- Lähnemann, D., Köster, J., Szczurek, E., McCarthy, D. J., Hicks, S. C., Robinson, M. D., Vallejos, C. A., Campbell, K. R., Beerenwinkel, N., Mahfouz, A. et al. (2020), ‘Eleven grand challenges in single-cell data science’, *Genome biology* **21**(1), 1–35.
- Leiner, J., Duan, B., Wasserman, L. & Ramdas, A. (2023), ‘Data fission: splitting a single data point’, *Journal of the American Statistical Association* pp. 1–12.
- Li, Q., Noel-MacDonnell, J. R., Koestler, D. C., Goode, E. L. & Fridley, B. L. (2018), ‘Subject level clustering using a negative binomial model for small transcriptomic studies’, *BMC bioinformatics* **19**(1), 1–10.
- MacQueen, J. et al. (1967), ‘Some methods for classification and analysis of multivariate observations’, **1**(14), 281–297.
- Neufeld, A., Dharamshi, A., Gao, L. L. & Witten, D. (2023), ‘Data thinning for convolution-closed distributions’, *arXiv preprint arXiv:2301.07276* .
- Neufeld, A., Gao, L. L., Popp, J., Battle, A. & Witten, D. (2024), ‘Inference after latent variable estimation for single-cell rna sequencing data’, *Biostatistics* **25**(1), 270–287.
- Neufeld, A., Popp, J., Gao, L. L., Battle, A. & Witten, D. (2023), ‘Negative binomial count splitting for single-cell rna sequencing data’, *arXiv preprint arXiv:2307.12985* .
- Pullin, J. M. & McCarthy, D. J. (2024), ‘A comparison of marker gene selection methods for single-cell rna sequencing data’, *Genome Biology* **25**(1), 56.
- Siffer, A., Fouque, P.-A., Termier, A. & LARGOUËT, C. (2018), Are your data gathered?, *in*

‘Proceedings of the 24th acm sigkdd international conference on knowledge discovery & data mining’, pp. 2210–2218.

Song, D., Li, K., Ge, X. & Li, J. J. (2023), ‘Clusterde: a post-clustering differential expression (de) method robust to false-positive inflation caused by double dipping’, *Research Square* .

Welch, B. L. (1947), ‘The generalization of ‘student’s’ problem when several different population variances are involved’, *Biometrika* **34**(1-2), 28–35.

Yun, Y.-J. & Foygel Barber, R. (2023), ‘Selective inference for clustering with unknown variance’, *Electronic Journal of Statistics* **17**(2), 1923–1946.

Zhang, J. M., Kamath, G. M. & David, N. T. (2019), ‘Valid post-clustering differential analysis for single-cell rna-seq’, *Cell systems* **9**(4), 383–392.

## A Independence proof of the Gaussian process

Let  $\mathbf{X} \sim \mathcal{N}(\boldsymbol{\mu}, \boldsymbol{\Sigma}_{p \times p})$ . Considering the fission process for Gaussian data described in Table 1, we can decompose  $\mathbf{X}$  into two new random variables  $\mathbf{X}^{(1)}$  and  $\mathbf{X}^{(2)}$  using a new random variable  $\mathbf{Z} \sim \mathcal{N}(\mathbf{0}, \boldsymbol{\Sigma})$ . It follows from this decomposition that:

$$\mathbf{X}^{(1)} \sim \mathcal{N}(\boldsymbol{\mu}, (1 + \tau^2) \boldsymbol{\Sigma}) \quad \text{and} \quad \mathbf{X}^{(2)} \sim \mathcal{N}\left(\boldsymbol{\mu}, \left(1 + \frac{1}{\tau^2}\right) \boldsymbol{\Sigma}\right)$$

Moreover, we have  $\mathbf{X}^{(1)} \perp\!\!\!\perp \mathbf{X}^{(2)}$ . Indeed, we have:

$$\begin{aligned}
\text{Cov}(\mathbf{X}^{(1)}, \mathbf{X}^{(2)}) &= \mathbb{E} \left[ \left( \mathbf{X}^{(1)} - \mathbb{E}[\mathbf{X}^{(1)}] \right) \left( \mathbf{X}^{(2)} - \mathbb{E}[\mathbf{X}^{(2)}] \right)^t \right] \\
&= \mathbb{E} \left[ \left( \mathbf{X}^{(1)} - \boldsymbol{\mu} \right) \left( \mathbf{X}^{(2)} - \boldsymbol{\mu} \right)^t \right] \quad \text{since} \quad \mathbb{E}[\mathbf{X}^{(1)}] = \mathbb{E}[\mathbf{X}^{(2)}] = \boldsymbol{\mu} \\
&= \mathbb{E} \left[ \mathbf{X}^{(1)} \mathbf{X}^{(2)t} - \mathbf{X}^{(1)} \boldsymbol{\mu}^t - \boldsymbol{\mu} \mathbf{X}^{(2)t} + \boldsymbol{\mu} \boldsymbol{\mu}^t \right] \\
&= \mathbb{E}[\mathbf{X}^{(1)} \mathbf{X}^{(2)t}] - \mathbb{E}[\mathbf{X}^{(1)}] \boldsymbol{\mu}^t - \boldsymbol{\mu} \mathbb{E}[\mathbf{X}^{(2)t}] + \boldsymbol{\mu} \boldsymbol{\mu}^t \\
&= \mathbb{E}[\mathbf{X}^{(1)} \mathbf{X}^{(2)t}] - \boldsymbol{\mu} \boldsymbol{\mu}^t - \boldsymbol{\mu} \boldsymbol{\mu}^t + \boldsymbol{\mu} \boldsymbol{\mu}^t \\
&= \mathbb{E}[\mathbf{X}^{(1)} \mathbf{X}^{(2)t}] - \boldsymbol{\mu} \boldsymbol{\mu}^t
\end{aligned}$$

Moreover, we have:

$$\begin{aligned}
\mathbb{E}[\mathbf{X}^{(1)} \mathbf{X}^{(2)t}] &= \mathbb{E} \left[ \left( \mathbf{X} + \tau \mathbf{Z} \right) \left( \mathbf{X} - \frac{1}{\tau} \mathbf{Z} \right)^t \right] \\
&= \mathbb{E} \left[ \mathbf{X} \mathbf{X}^t - \frac{1}{\tau} \mathbf{X} \mathbf{Z}^t + \tau \mathbf{Z} \mathbf{X}^t - \mathbf{Z} \mathbf{Z}^t \right] \\
&= \mathbb{E}[\mathbf{X} \mathbf{X}^t] - \frac{1}{\tau} \mathbb{E}[\mathbf{X} \mathbf{Z}^t] + \tau \mathbb{E}[\mathbf{Z} \mathbf{X}^t] - \mathbb{E}[\mathbf{Z} \mathbf{Z}^t] \\
&= \mathbb{E}[\mathbf{X} \mathbf{X}^t] - \frac{1}{\tau} \mathbb{E}[\mathbf{X}] \mathbb{E}[\mathbf{Z}^t] + \tau \mathbb{E}[\mathbf{Z}] \mathbb{E}[\mathbf{X}^t] - \mathbb{E}[\mathbf{Z} \mathbf{Z}^t] \quad \text{since} \quad \mathbf{X} \perp\!\!\!\perp \mathbf{Z} \\
&= \mathbb{E}[\mathbf{X} \mathbf{X}^t] - \mathbb{E}[\mathbf{Z} \mathbf{Z}^t] \quad \text{since} \quad \mathbb{E}[\mathbf{Z}] = 0
\end{aligned}$$

But we also have:

$$\begin{aligned}
\text{Var}(\mathbf{X}) &= \mathbb{E}[\mathbf{X} \mathbf{X}^t] - \mathbb{E}[\mathbf{X}] \mathbb{E}[\mathbf{X}^t] = \boldsymbol{\Sigma} \\
&\iff \mathbb{E}[\mathbf{X} \mathbf{X}^t] = \boldsymbol{\Sigma} + \mathbb{E}[\mathbf{X}] \mathbb{E}[\mathbf{X}^t] \\
&\iff \mathbb{E}[\mathbf{X} \mathbf{X}^t] = \boldsymbol{\Sigma} + \boldsymbol{\mu} \boldsymbol{\mu}^t \quad \text{since} \quad \mathbb{E}[\mathbf{X}] = \boldsymbol{\mu}
\end{aligned}$$

and

$$\begin{aligned}
\text{Var}(\mathbf{Z}) &= \mathbb{E}[\mathbf{Z}\mathbf{Z}^t] - \mathbb{E}[\mathbf{Z}]\mathbb{E}[\mathbf{Z}^t] = \Sigma \\
\iff \mathbb{E}[\mathbf{Z}\mathbf{Z}^t] &= \Sigma + \mathbb{E}[\mathbf{Z}]\mathbb{E}[\mathbf{Z}^t] \\
\iff \mathbb{E}[\mathbf{Z}\mathbf{Z}^t] &= \Sigma \quad \text{since} \quad \mathbb{E}[\mathbf{Z}] = 0
\end{aligned}$$

So finally,

$$\text{Cov}(\mathbf{X}^{(1)}, \mathbf{X}^{(2)}) = \mathbb{E}[\mathbf{X}\mathbf{X}^t] - \mathbb{E}[\mathbf{Z}\mathbf{Z}^t] - \boldsymbol{\mu}\boldsymbol{\mu}^t = \Sigma + \boldsymbol{\mu}\boldsymbol{\mu}^t - \Sigma - \boldsymbol{\mu}\boldsymbol{\mu}^t = 0 \quad (4)$$

## B Impact of covariance estimation under the independence between $\mathbf{X}^{(1)}$ and $\mathbf{X}^{(2)}$

Now, let suppose that we use  $\mathbf{Z} \sim \mathcal{N}(\mathbf{0}, \hat{\Sigma})$  to perform data fission. It follows from equation (4) that, since  $\text{Var}(\mathbf{Z}) = \hat{\Sigma}$ ,

$$\text{Cov}(\mathbf{X}^{(1)}, \mathbf{X}^{(2)}) = \Sigma - \hat{\Sigma}$$

## C Derivation of $t$ -test statistic under the null of no-cluster in the univariate data fission post-clustering setting

The fission process, as outlined in Table 1, gives:

$$X^{(1)} \sim \mathcal{N}(\mu, \sigma^2 + \tau^2 \hat{\sigma}^2) \quad \text{and} \quad X^{(2)} \sim \mathcal{N}\left(\mu, \sigma^2 + \frac{1}{\tau^2} \hat{\sigma}^2\right)$$

After applying k-means clustering to the  $n$  realizations of  $X^{(1)}$ , two clusters  $\hat{C}_1$  and  $\hat{C}_2$  are obtained. As  $X^{(1)}$  follows a Gaussian distribution, the k-means clustering splits it into



two parts  $X^{(1)}|C_k$ ,  $k = 1, 2$ , with the same size  $n/2$  and the same variance, forming two half-Gaussian distributions. It follows from the half-Gaussian distribution that:

$$\mathbb{E}[X^{(1)}|C_k] = \pm \sqrt{\frac{2(\sigma^2 + \tau^2\hat{\sigma}^2)}{\pi}} \quad (5)$$

where the sign depends on whether  $\hat{C}_k$  represents the truncation on the right or left side of  $\mu$ . Using (5), the mean differences between  $\hat{C}_1$  and  $\hat{C}_2$  is then given by  $\hat{\delta}_{X^{(1)}} = \left| \mathbb{E}[X^{(1)}|\hat{C}_2] - \mathbb{E}[X^{(1)}|\hat{C}_1] \right| = 2\sqrt{\frac{2}{\pi}(\sigma^2 + \tau^2\hat{\sigma}^2)}$ . Due to the k-means clustering, the two estimated clusters share the same intra-cluster variance. Following the same half-Gaussian arguments, this shared intra-cluster variance in  $X^{(1)}$  is given by:

$$s_{X^{(1)}}^2 = (\sigma^2 + \tau^2\hat{\sigma}^2) \left(1 - \frac{2}{\pi}\right)$$

In the post-clustering data fission setting, hypothesis testing is applied on the realizations of  $X^{(2)}$  using  $\hat{C}_1$  and  $\hat{C}_2$ . Our focus is on the mean differences  $\hat{\delta}_{X^{(2)}}$  between these two clusters and their shared intra-cluster variances  $s^2(X^{(2)})$  on  $X^{(2)}$ . These values depend on the ability to reproduce the clustering results on  $X^{(2)}$  which is quantified by  $\text{Cor}(X^{(1)}, X^{(2)})$ . Assuming the same clustering for  $X^{(2)}$  as for  $X^{(1)}$  implies the same truncation on  $X^{(2)}$ . In this case, because  $X^{(2)} \sim \mathcal{N}\left(\mu, \sigma^2 + \frac{1}{\tau^2}\hat{\sigma}^2\right)$ , we have:

$$\hat{\delta}_{X^{(2)}} = 2\sqrt{\frac{2}{\pi}\left(\sigma^2 + \frac{1}{\tau^2}\hat{\sigma}^2\right)}$$

However, considering that the cluster analysis is applied first to  $X^{(1)}$  and then transferred to  $X^{(2)}$ , we need to account for the correlation between  $X^{(1)}$  and  $X^{(2)}$ , leading to:

$$\begin{aligned} \hat{\delta}_{X^{(2)}} &= 2\sqrt{\frac{2}{\pi}\left(\sigma^2 + \frac{1}{\tau^2}\hat{\sigma}^2\right)} \times |\text{Cor}(X^{(1)}, X^{(2)})| \\ &= 2\sqrt{\frac{2}{\pi}\left(\sigma^2 + \frac{1}{\tau^2}\hat{\sigma}^2\right)} \times \left| \frac{(\sigma^2 - \hat{\sigma}^2)}{\sqrt{(\sigma^2 + \tau^2\hat{\sigma}^2) \times (\sigma^2 + \frac{1}{\tau^2}\hat{\sigma}^2)}} \right| \end{aligned}$$

This mean difference  $\hat{\delta}_{X^{(2)}}$  can be interpreted as a trade-off between how easily  $\hat{C}_1$  and  $\hat{C}_2$  can be reproduced on  $X^{(2)}$  and the mean differences that would be observed if they were perfectly reproduced on  $X^{(2)}$ . For the shared intra-cluster variance,  $s^2(X^{(2)})$  should approximate  $(\sigma^2 + \frac{1}{\tau^2}\hat{\sigma}^2)(1 - \frac{2}{\pi})$  when  $|\text{Cor}(X^{(1)}, X^{(2)})|$  is close to 1 (the scenario where we accurately replicate  $\hat{C}_1$  and  $\hat{C}_2$  on  $X^{(2)}$ ). In this situation, as the two estimated clusters are fully preserved, their variances precisely follow the half-Gaussian variance on  $X^{(2)}$ . Conversely, when  $|\text{Cor}(X^{(1)}, X^{(2)})|$  is close to 0 (indicating the inability to reproduce the clustering results on  $X^{(2)}$  due to its independence with  $X^{(1)}$ ),  $s^2(X^{(2)})$  should approximate  $\sigma^2 + \frac{1}{\tau^2}\hat{\sigma}^2$ , representing the entire variance of  $X^{(2)}$ . This is a consequence of the independence between  $X^{(1)}$  and  $X^{(2)}$  that leads to random clusters on  $X^{(2)}$ . Thus, these two considerations give:

$$s^2(X^{(2)}) = \left(\sigma^2 + \frac{1}{\tau^2}\hat{\sigma}^2\right) \left(1 - \frac{2}{\pi}\right) \text{Cor}(X^{(1)}, X^{(2)})^2 + \left(\sigma^2 + \frac{1}{\tau^2}\hat{\sigma}^2\right) \left(1 - (\text{Cor}(X^{(1)}, X^{(2)}))^2\right) \quad (6)$$

In the post-clustering inference setting, we are interested in testing a mean difference between the two estimated clusters  $\hat{C}_1$  and  $\hat{C}_2$ . So, the null hypothesis we are interested in is:

$$\mathcal{H}_0 : \mu_{C_1} = \mu_{C_2} \quad \text{vs} \quad \mathcal{H}_1 : \mu_{C_1} \neq \mu_{C_2}$$

Under the null,  $T_{\hat{C}_1, \hat{C}_2} = \frac{\overline{X_{\hat{C}_1}^{(2)}} - \overline{X_{\hat{C}_2}^{(2)}}}{\sqrt{\frac{\hat{s}_{\hat{C}_1}^2}{n_1} + \frac{\hat{s}_{\hat{C}_2}^2}{n_2}}}$  where  $\overline{X_{C_k}^{(2)}} = \frac{1}{n_k} \sum_{i \in C_k} x_i^{(2)}$ .

We assumed that the 2-means clustering results in clusters such that  $n_1 = n_2 = \frac{n}{2}$ . Moreover, using the half Gaussian argument, we supposed that  $\hat{C}_1$  and  $\hat{C}_2$  shares the same intra-cluster variances given by  $s^2(X^{(2)})$ . So,

$$\begin{aligned}
T_{\hat{C}_1, \hat{C}_2} &= \frac{\overline{X_{\hat{C}_1}^{(2)}} - \overline{X_{\hat{C}_2}^{(2)}}}{\sqrt{\frac{s^2(X^{(2)})}{\frac{n}{2}} + \frac{s^2(X^{(2)})}{\frac{n}{2}}}} \\
&= \frac{\overline{X_{\hat{C}_1}^{(2)}} - \overline{X_{\hat{C}_2}^{(2)}}}{\sqrt{\frac{4s^2(X^{(2)})}{n}}}
\end{aligned}$$

We want to compute the null distribution of  $T_{\hat{C}_1, \hat{C}_2}$ . Using the Central Limit theorem, we know that:

$$\overline{X_{\hat{C}_1}^{(2)}} - \overline{X_{\hat{C}_2}^{(2)}} \sim \mathcal{N} \left( \underbrace{\mathbb{E}[X^{(2)}|\hat{C}_1] - \mathbb{E}[X^{(2)}|\hat{C}_2]}_{\hat{\delta}_{X^{(2)}}}, \text{Var} \left( \overline{X_{\hat{C}_1}^{(2)}} - \overline{X_{\hat{C}_2}^{(2)}} \right) \right)$$

But,

$$\begin{aligned}
\text{Var} \left( \overline{X_{\hat{C}_1}^{(2)}} - \overline{X_{\hat{C}_2}^{(2)}} \right) &= \text{Var} \left( \overline{X_{\hat{C}_1}^{(2)}} \right) + \text{Var} \left( \overline{X_{\hat{C}_2}^{(2)}} \right) \quad \text{by independence} \\
&= 2 \text{Var} \left( \overline{X_{\hat{C}_1}^{(2)}} \right) \quad \text{because we assumed same intra-cluster variance} \\
&= \frac{2}{\left(\frac{n}{2}\right)^2} \sum_{i \in \hat{C}_1} \text{Var} \left( X_i^{(2)} | C_1 \right) \\
&= \frac{8}{n^2} \frac{n}{2} \text{Var} \left( X_1^{(2)} | C_1 \right) \\
&= \frac{4}{n} \text{Var} \left( X_1^{(2)} | C_1 \right) \\
&= \frac{4}{n} s^2(X^{(2)})
\end{aligned}$$

So,

$$\overline{X_{\hat{C}_1}^{(2)}} - \overline{X_{\hat{C}_2}^{(2)}} \sim \mathcal{N} \left( \hat{\delta}_{X^{(2)}}, \frac{4}{n} s^2(X^{(2)}) \right)$$

Finally, we have:

$$\begin{aligned}
\mathbb{E} \left[ T_{\hat{C}_1, \hat{C}_2} \right] &= \mathbb{E} \left[ \frac{\overline{X_{\hat{C}_1}^{(2)}} - \overline{X_{\hat{C}_2}^{(2)}}}{\sqrt{\frac{4s^2(X^{(2)})}{n}}} \right] \\
&= \frac{1}{\sqrt{\frac{4s^2(X^{(2)})}{n}}} \mathbb{E} \left[ \overline{X_{\hat{C}_1}^{(2)}} - \overline{X_{\hat{C}_2}^{(2)}} \right] \\
&= \frac{\hat{\delta}_{X^{(2)}}}{\sqrt{\frac{4s^2(X^{(2)})}{n}}}
\end{aligned}$$

and:

$$\begin{aligned}
\text{Var} \left( T_{\hat{C}_1, \hat{C}_2} \right) &= \text{Var} \left( \frac{\overline{X_{\hat{C}_1}^{(2)}} - \overline{X_{\hat{C}_2}^{(2)}}}{\sqrt{\frac{4s^2(X^{(2)})}{n}}} \right) \\
&= \frac{1}{\frac{4s^2(X^{(2)})}{n}} \text{Var} \left( \overline{X_{\hat{C}_1}^{(2)}} - \overline{X_{\hat{C}_2}^{(2)}} \right) \\
&= \frac{1}{\frac{4s^2(X^{(2)})}{n}} \frac{4s^2(X^{(2)})}{n} \\
&= 1
\end{aligned}$$

So,

$$T_{\hat{C}_1, \hat{C}_2} \stackrel{\mathcal{H}_0}{\sim} \mathcal{N} \left( \frac{\hat{\delta}_{X^{(2)}}}{\sqrt{\frac{4s^2(X^{(2)})}{n}}}, 1 \right)$$

Since we have,  $\hat{\delta}_{X^{(2)}} = 2\sqrt{\frac{2}{\pi}} \left( \sigma^2 + \frac{1}{\tau^2} \hat{\sigma}^2 \right) \times |\text{Cor} (X^{(1)}, X^{(2)})|$  and  $s^2(X^{(2)}) = \left( \sigma^2 + \frac{1}{\tau^2} \hat{\sigma}^2 \right) \left( 1 - \frac{2}{\pi} \right) \left( \text{Cor} (X^{(1)}, X^{(2)}) \right)^2 + \left( \sigma^2 + \frac{1}{\tau^2} \hat{\sigma}^2 \right) \left( 1 - \left( \text{Cor} (X^{(1)}, X^{(2)}) \right)^2 \right)$ , which can be simplified as  $\left( \sigma^2 + \frac{1}{\tau^2} \hat{\sigma}^2 \right) \left( 1 - \frac{2}{\pi} \text{Cor} (X^{(1)}, X^{(2)})^2 \right)$ , then:

$$\begin{aligned}
\frac{\widehat{\delta}_{X^{(2)}}}{\sqrt{\frac{4s^2(X^{(2)})}{n}}} &= \frac{2\sqrt{\frac{2}{\pi}} \left(\sigma^2 + \frac{1}{\tau^2}\widehat{\sigma}^2\right) \times |\text{Cor}(X^{(1)}, X^{(2)})|}{\sqrt{\frac{4\left(\sigma^2 + \frac{1}{\tau^2}\widehat{\sigma}^2\right) \left(1 - \frac{2}{\pi} \text{Cor}(X^{(1)}, X^{(2)})^2\right)}{n}}} \\
&= \frac{2\sqrt{\frac{2}{\pi}} \sqrt{\left(\sigma^2 + \frac{1}{\tau^2}\widehat{\sigma}^2\right)} \sqrt{\text{Cor}(X^{(1)}, X^{(2)})^2}}{2\sqrt{\left(\sigma^2 + \frac{1}{\tau^2}\widehat{\sigma}^2\right)} \sqrt{1 - \frac{2}{\pi} \text{Cor}(X^{(1)}, X^{(2)})^2}} \\
&\quad \frac{1}{\sqrt{n}} \\
&= \frac{\sqrt{n} \sqrt{\frac{2}{\pi} \text{Cor}(X^{(1)}, X^{(2)})^2}}{\sqrt{1 - \frac{2}{\pi} \text{Cor}(X^{(1)}, X^{(2)})^2}}
\end{aligned}$$

So, under  $\mathcal{H}_0$ ,

$$T_{\widehat{C}_1, \widehat{C}_2} \stackrel{\mathcal{H}_0}{\sim} \mathcal{N} \left( \frac{\sqrt{n} \sqrt{\frac{2}{\pi} \text{Cor}(X^{(1)}, X^{(2)})^2}}{\sqrt{1 - \frac{2}{\pi} \text{Cor}(X^{(1)}, X^{(2)})^2}}, 1 \right)$$

The associated Type I error rate for this test is given by  $1 - F(q_{\alpha/2}) + F(-q_{\alpha/2})$ , where  $F$  is the cumulative distribution function of  $\mathcal{N} \left( \frac{\sqrt{n} \sqrt{\frac{2}{\pi} \text{Cor}(X^{(1)}, X^{(2)})^2}}{\sqrt{1 - \frac{2}{\pi} \text{Cor}(X^{(1)}, X^{(2)})^2}}, 1 \right)$  (or the corresponding non-central  $\mathcal{T}(n-2)$  distribution), and  $q_{\alpha/2}$  is the quantile of a standard Gaussian distribution  $\mathcal{N}(0, 1)$  (or of a  $\mathcal{T}(n-2)$  distribution).